The accuracy of the quasi-LPV model has been validated in simulation across a flight envelope described by the variation ranges: $\alpha \in [0, 16]$ deg, $V \in [160, 280]$ m/s, $h \in [1, 15]$ km.

Aiming to employ the quasi-LPV model for the design of an LPV-based polytopic controller, a further modeling step has been necessary. Indeed, the obtained quasi-LPV model does not respect the affine model-parameter relation imposed by the polytopic formulation. Thus, a model approximation procedure has been developed, with the purpose to reformulate the projectile quasi-LPV model into a polytopic system. The approximation relies on the identification of a new set of scheduling functions, $\hat{\boldsymbol{\rho}}$ in Equation (2.38), affine w.r.t. the system dynamics.

Projectile Pitch Channel quasi-LPV/Polytopic Model. The approximation process results in the polytopic reformulation of the projectile quasi-LPV pitch channel dynamics, Σ_{PY}, defined in Equation (2.39) as follows:

$$\Sigma_{\text{PY}}: \begin{bmatrix} \dot{\alpha} \\ \dot{q}_{\text{dev}} \\ \dot{\delta}_{q,\text{dev}} \end{bmatrix} = \begin{bmatrix} 0 & 1 & \bar{A}_{13}(\hat{\rho}_1) \\ 0 & \bar{A}_{22}(\hat{\rho}_1) - \hat{\rho}_2 & \bar{A}_{23}(\hat{\rho}_1) \\ 0 & -\hat{\rho}_3 & -\hat{\rho}_3 \bar{A}_{13}(\hat{\rho}_1) \end{bmatrix} \begin{bmatrix} \alpha \\ q_{\text{dev}} \\ \delta_{q,\text{dev}} \end{bmatrix} + \begin{bmatrix} 0 \\ 0 \\ 1 \end{bmatrix} \sigma \tag{2.42}$$

where:

$$\hat{\rho}_1 \coloneqq \bar{q}; \qquad \hat{\rho}_2 \coloneqq \frac{\partial q_{\text{eq}}}{\partial \alpha}; \qquad \hat{\rho}_3 \coloneqq \frac{\partial \delta_{q,\text{eq}}}{\partial \alpha}$$

and:

$$\bar{A}_{13}(\hat{\rho}_1) = \frac{\bar{q}S}{m\bar{V}} \bar{C}_{Z_{\delta_{q1}}}; \qquad \bar{A}_{22}(\hat{\rho}_1) = \frac{\bar{q}Sd}{I_2} \left(\frac{d}{2\bar{V}} \right) \bar{C}_{m_q}; \qquad \bar{A}_{23}(\hat{\rho}_1) = \frac{\bar{q}Sd}{I_2} \bar{C}_{m_{\delta_{q1}}}.$$

Concerning the output equation, the output matrix, $\mathcal{C}$, consists of the identity matrix, $I \in \mathbb{R}^{3\times 3}$, assuming a state feedback architecture. The feedforward matrix, $\mathcal{D}$, is assumed zero.

After assessing the accuracy of the approximation process, the original domain of validity of the quasi-LPV model has been mapped into the new convex polytope, $\hat{\Theta}$, defined by the scheduling functions: $\hat{\rho}_1(V, h) \in [0.4,\ 2.9] \times 10^4$, $\hat{\rho}_2(\alpha, V, h) \in [0.05,\ 0.55]$, and $\hat{\rho}_3(\alpha, V, h) \in [-1,\ 4.1]$. In the next chapter, the projectile quasi-LPV model, and the corresponding polytopic approximation, will be used respectively for the design of grid-based and polytopic LPV autopilot. The performance of the two design approaches will be deeply investigated and compared.

Part II

Projectile Autopilot Design: LPV-based robust controller design approaches for guided munitions

Chapter 3

LPV Controller Design

Contents

3.1 Introduction

The synthesis of LPV controllers relies on the resolution of convex optimization problems, formulated as linear matrix inequalities (LMIs). Different from standard LTI gain-scheduling strategies, the design guarantees relevant stability properties not only in the vicinity of a selected set of operating conditions but also across the transient phase. Indeed, the gain-scheduling design is often based on the online interpolation of a set of independently designed LTI local controllers. As a consequence, no guarantees are provided concerning the performance of the interpolated controller, especially in the case of sharp variations in the operating conditions. By limiting the admissible variation range of each operating parameter ('slow variation' assumption as discussed in [SA92]), stability performance can be recovered in the transition between two steady-state conditions, at the expense of significant restrictions on the range of applications ([RS00]).

In the LPV framework, higher stability guarantees and performance can be obtained depending on the formulation of the LMIs optimization problem. Due to the continuous variation of the parameters, the optimization problem results in an unfeasible infinite number of conditions. Through the imposition of an affine model-parameter relation, the optimization can be solved across a convex (polytope) subspace defined by the ranges of variation of the parameters. By exploiting the linear variation of the parameters, the design ensures stability guarantees across the polytope. Alternatively, the continuous space of variation of the parameters can be discretized into a finite set of design conditions (gridding). By additionally accounting for the rate of variation of each parameter, the optimization problem can be further constrained, improving the performance of the resulting controller.

In this chapter, the aforementioned approaches are employed for the synthesis of a robust LPV autopilot for the projectile pitch channel dynamics, based on the $\mathcal{H}_\infty$ criterion. The former polytopic approach ensures broader stability guarantees at the expense of a more conservative optimization performance ([AGB95]; [SGC97]). The conservatism of the approach is targeted through the optimization of the polytope's dimensions and the consistency of the operating conditions belonging to the convex subset ([Jin+18]; [Kap+22]; [ZZW14]; [Cor+20]; [PDP05]; [Pan+21]; [HW15]; [KW08]). Conversely, the grid-based formulation, improves the optimization performance of the controller synthesis, even though the stability guarantees in the transient between different design points are weaker than the polytopic case ([WPB95]; [Wu+96]). However, by simultaneously satisfying the LMIs at all the grid conditions through a parameter-dependent solution, the likelihood of reliable performance related to the controller interpolation is much higher than in the standard LTI gain-scheduling approach.

The chapter is structured in the following sections:

S3.2: recalls the fundamental concepts related to the stability properties of different classes of LPV systems. The LPV-based controller synthesis is formulated as an LMIs optimization problem that aims at minimizing the induced L_2-norm of the system. The conditions related to the resolution of the LMIs optimization through the polytopic and grid-based approaches are finally detailed.

S3.3: focuses on the design of an LPV autopilot for the projectile pitch channel dynamics, based on the polytopic approach. The control scheme is first introduced by addressing the core objectives of the design. The conservatism affecting the controller synthesis is addressed by analyzing the variation of the scheduling functions across the selected convex space. The results of the design are finally investigated in the frequency domain. The results presented in this section have been published in [Vin+23a]; [Vin+23b].

S3.4: discusses the resolution of the LPV controller synthesis, by gridding the scheduling variables space. An output feedback configuration is employed for the design of the grid-based autopilot for the projectile pitch channel dynamics. The gridding process is extensively investigated in order to optimize the performance of the controller synthesis. As for the polytopic case, the results of the design are analyzed in the frequency domain. The results presented in this section have been published in [Vin+23c].

3.2 Fundamentals on LPV Control Design

This section provides a brief and non-exhaustive overview concerning the different notions of stability properties for LPV systems and the conditions that have been developed to assess the degree of stability of a generic LPV system. Finally, the synthesis of LPV-based controllers is formulated in terms of feasible optimization problems. Further information can be found in [Boy+94]; [Bri14]; [MS12]; [SGB13].

3.2.1 Linear Matrix Inequalities

The resolution of linear matrix inequalities (LMIs) systems represents a fundamental tool in the formulation of convex optimization problems, such as the synthesis of LPV controllers.

Definition 3.1 (Linear Matrix Inequalities (LMIs))
A linear matrix inequality consists of a compact formulation to express an algebraic convex constraint on a generic vector $\boldsymbol{x} \in \mathbb{R}^N$*, as:*

$$\mathcal{L}(\boldsymbol{x}) \coloneqq \mathcal{L}_0 + \sum_{i=1}^{N} \mathcal{L}_i x_i \succeq 0 \tag{3.1}$$

where $\mathcal{L}_0 = \mathcal{L}_0^{\mathrm{T}}$*, and* $\mathcal{L}_i = \mathcal{L}_i^{\mathrm{T}} \in \mathbb{R}^{N \times N}$ *are known matrices. The constraint can impose a symmetric and positive semi-definite matrix condition,* $\mathcal{L} \succeq 0$*, or a positive definite matrix condition,* $\mathcal{L} \succ 0$*. In the latter case, it is referred to as 'strict' LMI.*
The solution of an LMIs problem consists of finding a convex set, $\mathbb{L}$*, defined by all the possible vectors,* $\boldsymbol{x}$*, that satisfy the constraint in Equation* (3.1)*:*

$$\mathbb{L} = \{\boldsymbol{x} \in \mathbb{R}^N | \mathcal{L}(\boldsymbol{x}) \succeq 0 \ (\text{or} \succ 0)\}.$$

In control applications, LMIs as in Definition 3.1 are employed to target the location of the eigenvalues of $\mathcal{L}$, imposing either positive $\mathcal{L} \succ 0$, or negative values, $\mathcal{L} \prec 0$. In particular, multiple LMIs constraints can be formulated as a single condition, as follows:

$$\mathcal{L}(\boldsymbol{x}) = \begin{pmatrix} \mathcal{L}^1(\boldsymbol{x}) & 0 & \cdots & 0 \\ 0 & \mathcal{L}^2(\boldsymbol{x}) & \cdots & 0 \\ \vdots & \vdots & \ddots & \vdots \\ 0 & 0 & \dots & \mathcal{L}^k(\boldsymbol{x}) \end{pmatrix} \tag{3.2}$$

The solution of the system in Equation (3.2) is given by the union of the eigenvalues of the individual matrices, $\mathcal{L}^j(\boldsymbol{x})$ with $j = 1, \dots, k$. Since it consists of the intersection of multiple convex sets, the solution of the system in Equation (3.2) defines also a convex set.

Systems of inequalities defined as in Equation (3.2) represent a standard formulation for convex control design optimization problems. Depending on the constraints imposed through the definition of the LMIs, optimization problems can be classified as in the following.

Definition 3.2 (Semi-Definite Programming LMIs Problem (SDP))
A semi-definite LMIs optimization programming problem is formally defined as:

$$\begin{aligned} &\min \boldsymbol{c}^{\mathrm{T}}\boldsymbol{x} \\ &\quad \text{s.t. } \boldsymbol{x} \in \mathbb{R}^N \\ &\qquad \mathcal{L}(\boldsymbol{x}) \succ 0 \end{aligned}$$

where $\boldsymbol{c} \in \mathbb{R}^N$.

Definition 3.3 (Semi-Infinite LMIs Problem)
A semi-infinite LMIs optimization problem is formally defined as:

$$\begin{aligned} &\min \boldsymbol{c}^{\mathrm{T}}\boldsymbol{x} \\ &\quad \text{s.t. } \boldsymbol{x} \in \mathbb{R}^N \\ &\mathcal{L}(\boldsymbol{x}, \boldsymbol{\rho}) \coloneqq \mathcal{L}_0(\boldsymbol{\rho}) + \sum_{i=1}^{N} \mathcal{L}_i(\boldsymbol{\rho}) x_i \succeq 0; \qquad \textit{with} \quad \boldsymbol{\rho} \in \mathbb{U}_\rho \end{aligned}$$

where $\boldsymbol{c} \in \mathbb{R}^N$, *and* $\mathbb{U}_\rho \in \mathbb{R}^{n_\rho}$ *is a compact set.*

Definition 3.4 (Infinite-Dimensional LMIs Problem)
An infinite-dimensional LMIs optimization problem is formally defined as:

$$\begin{aligned} &\min \boldsymbol{c}^{\mathrm{T}}\boldsymbol{x}(\boldsymbol{\rho}) \\ &\quad \text{s.t. } \boldsymbol{x} : \mathbb{U}_\rho \to \mathbb{R}^N \\ &\mathcal{L}(\boldsymbol{x}(\boldsymbol{\rho}), \boldsymbol{\rho}) \coloneqq \mathcal{L}_0(\boldsymbol{\rho}) + \sum_{i=1}^{N} \mathcal{L}_i(\boldsymbol{\rho}) x_i(\boldsymbol{\rho}) \succeq 0; \qquad \textit{with} \quad \boldsymbol{\rho} \in \mathbb{U}_\rho \end{aligned}$$

where $\boldsymbol{c} \in \mathbb{R}^N$, $\mathbb{U}_\rho \in \mathbb{R}^{n_\rho}$ *is a compact set, and* $\boldsymbol{x} : \mathbb{U}_\rho \to \mathbb{R}^N$ *is a parameter-dependent function.*

Several optimization tools have been developed in the past years to solve SDP LMIs problems in Definition 3.2, such as Yalmip ([Lof04]) and CVX ([GB08]), equipped with sophisticated solver algorithms (e.g. SDPT3, Mosek, and SeDuMi). Differently, in semi-infinite and infinite-dimensional LMIs problems, the constraints are parameter-dependent, meaning that the corresponding LMIs have to be satisfied for an infinite number of conditions, defined by the continuous variation of the parameters, $\boldsymbol{\rho} \in \mathbb{U}_\rho$. As detailed in the next section, semi-infinite LMIs optimization problems can be converted into solvable SDP problems by means of standard matrix relaxation techniques. Instead, the solution of an infinite-dimensional LMIs problem requires a first reformulation as a semi-infinite problem by converting the infinite parameter-dependent decision variables, $\boldsymbol{x}(\boldsymbol{\rho})$, into a finite set. Then, the resulting semi-infinite problem is addressed through relaxation techniques, as previously mentioned.

3.2.2 Stability of LPV Systems

This section recalls the basic concepts concerning the stability conditions of different classes of LPV systems. The stability of LPV systems is achieved through the imposition of a set of constraints on the eigenvalues of the system state matrix, in the form of LMIs conditions. In particular, it relies on the extension to the LPV framework of the well-established Lyapunov definition of system equilibrium properties, and the corresponding Lyapunov's Stability Theorem of dynamical systems, discussed in [Lya92]; [Kha02].

Lyapunov Stability. Without loss of generality, from the general formulation in Equation (2.2) assume the autonomous LPV continuous dynamics, given by:

$$\begin{aligned} &\dot{\boldsymbol{x}}(t) = \mathcal{A}(\boldsymbol{\rho}(t))\boldsymbol{x}(t); \qquad \text{with: } \boldsymbol{x}(t) \in \mathbb{R}^{n_x};\ \boldsymbol{\rho}(t) \in \mathbb{R}^{n_\rho};\ t \geq 0 \\ &\boldsymbol{x}(0) = \boldsymbol{x}_0. \end{aligned} \tag{3.3}$$

From Lyapunov theory, the stability of the parameter-varying system in Equation (3.3) relies on the identification of a Lyapunov function:

$$V(\boldsymbol{x}) \coloneqq \boldsymbol{x}^{\mathrm{T}} P \boldsymbol{x}; \qquad \text{with: } P \in \mathbb{R}^{n_x \times n_x} \succ 0$$

such that the derivative, $\dot{V}(\boldsymbol{x}, \boldsymbol{\rho})$, satisfies the following Lyapunov condition:

$$\dot{V}(\boldsymbol{x}, \boldsymbol{\rho}) \coloneqq \boldsymbol{x}(t)^{\mathrm{T}} \left(\mathcal{A}(\boldsymbol{\rho})^{\mathrm{T}} P + P \mathcal{A}(\boldsymbol{\rho}) \right) \boldsymbol{x}(t) \prec 0 \tag{3.4}$$

for all the parameters' trajectories, $\boldsymbol{\rho} \in \mathbb{R}^{n_\rho}$.

In particular, depending on the parameterization of the selected Lyapunov function, the conditions expressed in Equation (3.4) can be reformulated providing different guarantees of stability ([Bri14]).

Definition 3.5 (Quadratic Stability)
The system in Equation (3.3) *is said to be quadratically stable if there exists a parameter-independent Lyapunov function,* $V(\boldsymbol{x}) = \boldsymbol{x}^{\mathrm{T}} P \boldsymbol{x} \succ 0$ *for every* $\boldsymbol{x} \neq 0$, *and* $V(0) = 0$, *that satisfies the Lyapunov condition in Equation* (3.4), *reformulated as:*

$$\mathcal{A}(\boldsymbol{\rho})^{\mathrm{T}} P + P \mathcal{A}(\boldsymbol{\rho}) \prec 0$$

for every $\boldsymbol{x} \neq 0$, *and such that* $\dot{V}(0, \boldsymbol{\rho}) = 0$ *for every* $\boldsymbol{\rho} \in \mathbb{R}^{n_\rho}$.

Definition 3.6 (Robust Stability)
The system in Equation (3.3) *is said to be robustly stable if there exists a parameter-dependent Lyapunov function,* $V(\boldsymbol{x}, \boldsymbol{\rho}) = \boldsymbol{x}^{\mathrm{T}} P(\boldsymbol{\rho}) \boldsymbol{x} \succ 0$ *for every* $\boldsymbol{x} \neq 0$, *and* $V(0) = 0$, *that satisfies the Lyapunov condition in Equation* (3.4), *reformulated as:*

$$\mathcal{A}(\boldsymbol{\rho})^{\mathrm{T}} P(\boldsymbol{\rho}) + P(\boldsymbol{\rho}) \mathcal{A}(\boldsymbol{\rho}) + \sum_{i=1}^{n_\rho} \dot{\rho}_i \frac{\partial P(\boldsymbol{\rho})}{\partial \rho_i} \prec 0$$

for every $\boldsymbol{x} \neq 0$, *and such that* $\dot{V}(0, \boldsymbol{\rho}) = 0$ *for every* $\boldsymbol{\rho} \in \mathbb{R}^{n_\rho}$.

Remark 3.1
The definition of quadratic stability does not account for bounded rates of variation of the parameters, $\dot{\boldsymbol{\rho}}$, possibly resulting in a very conservative condition to be satisfied. Indeed, it represents a sufficient but not necessary condition for asymptotic stability ([Bri14]). Differently, robust stability distinguishes between slow and fast-varying parameters, providing less conservatism in the formulation of the constraints, but also lower global guarantees of stability. In reason of these definitions, quadratic stability implies robust stability, but not vice versa. Indeed, the derivative of the Lyapunov function is not guaranteed to be negative definite for all ($\boldsymbol{\rho}$, $\dot{\boldsymbol{\rho}}$) conditions because of the additional terms:

$$\sum_{i=1}^{n_\rho} \dot{\rho}_i \frac{\partial P(\boldsymbol{\rho})}{\partial \rho_i}.$$

The assessment of quadratic and robust stability of LPV systems relies on the formulation of the semi-infinite and infinite-dimensional LMIs problems, introduced in Definition 3.3 and Definition 3.4, respectively. In the following, the robust stability of a generic LPV system is addressed through the projection of the infinite-dimensional LMIs decision variables into a set of finite-dimensional basis functions. The resulting semi-infinite problem is solved through the relaxation of the LMIs conditions by gridding the parameters' space. Concerning the feasibility of the quadratic stability conditions, the reformulation of the LPV system in Equation (3.3) as a polytopic model allows exploiting the advantages of the affine-parameter dependence in the resolution of convex optimization problems. The alternative gridding approach is not detailed in the presence work for brevity.

3.2.2.1 Robust Stability via Gridding Approach

The resolution of the infinite-dimensional LMIs problem that guarantees robust stability in the sense of Definition 3.6 can be achieved through the projection of the parameter-dependent matrix, $P(\boldsymbol{\rho}) = P(\boldsymbol{\rho})^{\mathrm{T}} \succ 0$, on a set of scalar basis functions, $f_i(\boldsymbol{\rho})$ with $i = 1, \ldots, n_{\mathrm{B}}$. Based on the selection of $f_i(\boldsymbol{\rho})$, the parameter-dependent matrix can be parameterized as:

$$P(\boldsymbol{\rho}) = \sum_{i=1}^{n_{\mathrm{B}}} P_i f_i(\boldsymbol{\rho})$$

where the new set of decision variables, corresponding to the matrices $P_i = P_i^{\mathrm{T}}$, has a finite dimension. As a consequence, the robust stability condition in Definition 3.6 can be expressed as in the following theorem.

Theorem 3.1
The LPV system formulated in Equation (3.3) *is robustly stable if there exist matrices* $P_i = P_i^{\mathrm{T}}$

such that the following LMIs:

$$\mathcal{A}(\boldsymbol{\rho})^{\mathrm{T}}\left(\sum_{i=1}^{n_{\mathrm{B}}} P_i f_i(\boldsymbol{\rho})\right)+\left(\sum_{i=1}^{n_{\mathrm{B}}} P_i f_i(\boldsymbol{\rho})\right)\mathcal{A}(\boldsymbol{\rho})+\sum_{i=1}^{n_\rho}\nu_i\left(\sum_{i=1}^{n_{\mathrm{B}}} P_i\frac{\partial f_i(\boldsymbol{\rho})}{\partial \rho_i}\right)\prec 0$$

$$\sum_{i=1}^{n_{\mathrm{B}}} P_i f_i(\boldsymbol{\rho})\succ 0$$

hold for all $\boldsymbol{\rho}\in\mathbb{U}_\rho$, *where* $\mathbb{U}_\rho\in\mathbb{R}^{n_\rho}$ *is a compact set, and all the vertices of the polytope,* $\nu=\underset{i=1}{\overset{n_\rho}{\mathrm{col}}}(\nu_i)$, *where the parameters' derivative,* $\dot{\boldsymbol{\rho}}$, *evolves.*

Remark 3.2
The selection of the set of basis functions, $f_i(\boldsymbol{\rho})$, *is not restricted to any specific parameter dependence. Thus, the projection approach can be applied to all classes of LPV systems. However, the higher the number of selected functions,* n_{B}, *the higher the computational complexity affecting the resolution of the LMIs problem. Additionally, no standard criteria are provided for the selection of the basis functions. Generally, it relies on the mimic principle, where the functions are chosen in a way to replicate the same model-parameter dependence presented by the LPV system ([AA98]).*

Through the reformulation discussed in Theorem 3.1, the infinite-dimensional robust stability LMIs problem has been converted into a semi-infinite problem. The last conversion step consists of the relaxation of the infinite number of parameter-varying LMIs to be solved. A standard solution relies on the discretization of the continuous space of variation of the parameters into a finite grid of n_{g} selected values, $\boldsymbol{\rho}\in\bar{\mathbb{U}}_\rho\coloneqq\{\boldsymbol{\rho}^1,\ldots,\boldsymbol{\rho}^{n_{\mathrm{g}}}\}$. Thus, the semi-infinite LMIs condition in Theorem 3.1 can be reformulated as:

Proposition 3.1
The LPV system in Equation (3.3) *is robustly stable if there exists matrices* $P_i=P_i^{\mathrm{T}}$ *such that the LMIs:*

$$\mathcal{A}(\boldsymbol{\rho})^{\mathrm{T}}\left(\sum_{i=1}^{n_{\mathrm{B}}} P_i f_i(\boldsymbol{\rho})\right)+\left(\sum_{i=1}^{n_{\mathrm{B}}} P_i f_i(\boldsymbol{\rho})\right)\mathcal{A}(\boldsymbol{\rho})+\sum_{i=1}^{n_\rho}\nu_i\left(\sum_{i=1}^{n_{\mathrm{B}}} P_i\frac{\partial f_i(\boldsymbol{\rho})}{\partial \rho_i}\right)\prec 0$$

$$\sum_{i=1}^{n_{\mathrm{B}}} P_i f_i(\boldsymbol{\rho})\succ 0$$

hold for all the n_{g} *values of* $\boldsymbol{\rho}\in\bar{\mathbb{U}}_\rho$, *where* $\bar{\mathbb{U}}_\rho\coloneqq\{\boldsymbol{\rho}^1,\ldots,\boldsymbol{\rho}^{n_{\mathrm{g}}}\}$, *and all the vertices of the polytope,* $\nu=\underset{i=1}{\overset{n_\rho}{\mathrm{col}}}(\nu_i)$, *where the parameters' derivative,* $\dot{\boldsymbol{\rho}}$, *evolves.*

Remark 3.3
The resolution of the LMIs optimization through grid-based relaxation consists of an approximation of the LMIs problem in Theorem 3.1. A major drawback related to this technique relies on the lack of guidelines for the optimal selection of the grid points during the discretization. Indeed, the selection of an optimal grid that ensures capturing the most significant and criti-

cal parameters' values, implies the prior knowledge of the feasible/unfeasible conditions of the optimization problem itself, generating a paradox.

A relevant consequence inferred from Remark 3.3 concerns the lack of guarantees about the system dynamics variation between the grid points. The selection of a denser and unevenly discretized grid can increase the likelihood of imposing stable conditions in the transient dynamics between known points. However, the computational complexity related to the resolution of the LMIs problem tends to increase with the number of grid points as $\mathcal{O}({n_g}^{n_\rho})$. Thus, depending on the application, ad-hoc solutions might be necessary for an accurate identification of the critical areas of the parameters' space.

3.2.2.2 Quadratic Stability via Polytopic Formulation

An alternative solution for the conversion of a semi-infinite LMIs problem into a solvable SDP one consists of the reformulation of the LPV system as a polytopic model.

The polytopic formulation presented in Section 2.2.1.1 relies on the affine model-parameter dependence assumption expressed in Definition 2.4. Without loss of generality, assume the LPV autonomous system in Equation (3.3), expressed in the polytopic formulation presented in Equation (2.4), and accounting for $n_\Theta = 2^{n_\rho}$, as:

$$\begin{aligned} \dot{\boldsymbol{x}}(t) &= \sum_{i=1}^{2^{n_\rho}} \mu_{\theta_i}(t)\mathcal{A}_i\boldsymbol{x}(t); \qquad \text{with:} \quad \boldsymbol{\rho} = \sum_{i=1}^{2^{n_\rho}} \mu_{\theta_i}\boldsymbol{\theta}_i \\ \boldsymbol{x}(0) &= \boldsymbol{x}_0 \end{aligned} \tag{3.5}$$

where the scheduling parameters, $\boldsymbol{\rho}(t) \in \mathbb{R}^{n_\rho}$, belong to the polytope, Θ, defined by the convex hull of the finite set of vertices, $\mathcal{V} = [\boldsymbol{\theta}_i, \ldots, \boldsymbol{\theta}_{2^{n_\rho}}]$. The interpolation variables, μ_{θ_i}, define the corresponding unitary polytope:

$$\Gamma := \left\{ \underset{i}{\text{col}}(\mu_{\theta_i}(t)) : \sum_{i=1}^{2^{n_\rho}} \mu_{\theta_i}(t) = 1,\ \mu_{\theta_i}(t) \geq 0 \right\}$$

Based on this assumption, the convexity of the polytope can be exploited by observing that, if the LMIs condition in Equation (3.4) holds for all of the vertices, $\boldsymbol{\theta}_i \in \mathcal{V}$, such that:

$$\mathcal{A}_i^{\mathrm{T}} P + P\mathcal{A}_i \prec 0$$

the corresponding sum of negative-definite matrices:

$$\sum_{i=1}^{2^{n_\rho}} \mu_{\theta_i} \left[\mathcal{A}_i^{\mathrm{T}} P + P\mathcal{A}_i\right]$$

is also negative-definite for all $\mu_{\theta_i} \in \Gamma$. Then, the quadratic stability condition presented in Definition 3.5 can be equivalently formulated as in the following.

Theorem 3.2
The LPV polytopic system in Equation (3.5) *is quadratically stable in the sense of Definition 3.5, if and only if there exists a matrix* $P = P^{\mathrm{T}} \succ 0$ *such that the LMI:*

$$\mathcal{A}_i^{\mathrm{T}} P + P\mathcal{A}_i \prec 0$$

holds for all $i = 1, \ldots, 2^{n_\rho}$.

The polytopic formulation allows converting the semi-infinite LMIs problem in Definition 3.5 into the equivalent finite number of 2^{n_ρ} conditions in Theorem 3.2, feasible for semi-definite programming computation.

Remark 3.4
Despite the feasibility of Theorem 3.2, the number of LMI conditions to be satisfied grows exponentially w.r.t. the number of scheduling variables, as $\mathcal{O}(2^{n_\rho})$. *Thus, the higher the dimension of* $\boldsymbol{\rho}(t)$, *the higher the computational complexity related to the stability assessment.*

As mentioned in Remark 3.4, quadratic stability tends to result in a generally conservative condition. Indeed, a common constant Lyapunov matrix, P, has to satisfy contemporary the LMIs at each vertex of the convex space of the parameters' variations. Additionally, the rates of variation of the scheduling parameters are not accounted for in the formulation. The robust stability condition introduced in Theorem 3.1 relies on parameter-varying Lyapunov matrices that can more optimally target the stability of the system at each parameter condition. The definition of robust stability for polytopic systems is not immediate since it requires the additional definition of the convex set of variation of the parameters' derivative, $\dot{\boldsymbol{\rho}}$. A standard solution, which is not detailed here, is based on the employment of slack-variables, introduced in [DOBG99]; [DOGH99] for discrete-time systems and then extended to the continuous case, as in [ATB01].

3.2.3 LPV Control Synthesis Problem

The criteria defined in the previous section, in the form of LMIs optimization problems, can be used to formulate the synthesis of a controller that guarantees certain stability and performance properties of the resulting closed-loop system. In particular, control systems can be classified based on the purpose they are designed to achieve, as:

- **Regulator:** targets the attenuation of external and internal disturbance signals that may affect the input or the output of the system.
- **Servo:** aims to follow a selected external reference signal, which guarantees the accomplishments of specific objectives.

For control-oriented purposes, the LPV state space representation introduced in Definition 2.2 of the previous chapter can be generalized, thus emphasizing the objectives targeted through

the control design, and distinguishing between the different inputs the model is subjected to. Indeed, the dynamics of any closed-loop system is generally affected by additional sources of internal and external disturbances, that can significantly deteriorate the performance of the controller, if not properly compensated. Model uncertainties, deriving from approximation processes or an inaccurate estimation of specific parameters, are typical examples of internal sources of disturbance. Instead, external disturbances are generally associated with the operating conditions of the system. In terms of aerospace applications, launch conditions and undesired wind contributions are generally accounted for as major sources of external disturbances. As a consequence, a more detailed state space representation of a general LPV model is employed for the formulation of the control synthesis problem.

Definition 3.7 (Generalized LPV System)
Given the vector of time-varying parameters, $\boldsymbol{\rho}(t) \in \mathbb{U}_\rho$, where $\mathbb{U}_\rho \in \mathbb{R}^{n_\rho}$ is a compact set, and $|\dot{\boldsymbol{\rho}}(t)| < \{\nu_i\}_{i=1}^{n_\rho}$ evolves in a convex polytope of bounded ranges, and given the set of parameter-varying matrices $\mathcal{A}(\boldsymbol{\rho}) \in \mathbb{R}^{n_{x_\mathrm{P}} \times n_{x_\mathrm{P}}}$, $\mathcal{B}_1(\boldsymbol{\rho}) \in \mathbb{R}^{n_{x_\mathrm{P}} \times n_w}$, $\mathcal{B}_2(\boldsymbol{\rho}) \in \mathbb{R}^{n_{x_\mathrm{P}} \times n_u}$, $\mathcal{C}_1(\boldsymbol{\rho}) \in \mathbb{R}^{n_z \times n_{x_\mathrm{P}}}$, $\mathcal{C}_2(\boldsymbol{\rho}) \in \mathbb{R}^{n_y \times n_{x_\mathrm{P}}}$, $\mathcal{D}_{11}(\boldsymbol{\rho}) \in \mathbb{R}^{n_z \times n_w}$, $\mathcal{D}_{12}(\boldsymbol{\rho}) \in \mathbb{R}^{n_z \times n_u}$, $\mathcal{D}_{21}(\boldsymbol{\rho}) \in \mathbb{R}^{n_y \times n_w}$, and $\mathcal{D}_{22}(\boldsymbol{\rho}) \in \mathbb{R}^{n_y \times n_u}$, the generalized LPV system, Σ_P, is formulated as:

$$\Sigma_\mathrm{P} : \begin{bmatrix} \dot{\boldsymbol{x}}_\mathrm{P}(t) \\ \hline \boldsymbol{z}(t) \\ \boldsymbol{y}(t) \end{bmatrix} = \left[\begin{array}{c|cc} \mathcal{A}(\boldsymbol{\rho}) & \mathcal{B}_1(\boldsymbol{\rho}) & \mathcal{B}_2(\boldsymbol{\rho}) \\ \hline \mathcal{C}_1(\boldsymbol{\rho}) & \mathcal{D}_{11}(\boldsymbol{\rho}) & \mathcal{D}_{12}(\boldsymbol{\rho}) \\ \mathcal{C}_2(\boldsymbol{\rho}) & \mathcal{D}_{21}(\boldsymbol{\rho}) & \mathcal{D}_{22}(\boldsymbol{\rho}) \end{array}\right] \begin{bmatrix} \boldsymbol{x}_\mathrm{P}(t) \\ \hline \boldsymbol{w}(t) \\ \boldsymbol{u}(t) \end{bmatrix}$$

where $\boldsymbol{x}_\mathrm{P}(t) \in \mathbb{R}^{n_{x_\mathrm{P}}}$ represents the state vector of the system, $\boldsymbol{w}(t) \in \mathbb{R}^{n_w}$ corresponds to the vector of exogenous inputs, $\boldsymbol{u}(t) \in \mathbb{R}^{n_u}$ stands for the vector of control inputs, $\boldsymbol{z}(t) \in \mathbb{R}^{n_z}$ includes the controlled outputs signals, targeting the design objectives, and $\boldsymbol{y}(t) \in \mathbb{R}^{n_y}$ is the vector of measured outputs.

Remark 3.5
The definition of the exogenous input vector, $\boldsymbol{w}(t)$, and of the controlled output vector, $\boldsymbol{z}(t)$, is not related to the state vector partition in the scheduling and non-scheduling subsets introduced in the quasi-LPV system Definition 2.2 of Chapter 2. Coherently, the partitions of the matrices $\mathcal{A}$, $\mathcal{B}$, $\mathcal{C}$, and $\mathcal{D}$ are not the same as the ones in Definition 2.2.

The employment of design methods in the robust control framework guarantees the capability ('robustness') of the resulting closed-loop system to handle any deviations from its ideal nominal operating conditions. The stability and performance objectives of the control design are distinguished into nominal, NS/NP (not accounting for disturbances), and robust, RS/RP (accounting for a certain level of disturbances). In this framework, a standard design approach consists of the $\mathcal{H}_\infty$ synthesis.

3.2.3.1 $\mathcal{H}_\infty$ Design Criterion

The effect of the input disturbances on the system dynamics can be quantified in terms of the amplification observed in the output signal energy, induced by the energy associated with the

disturbance signal. This amplification is defined through the evaluation of the system induced L_2-norm ([BP94]).

Definition 3.8 (Induced L_2-norm ([Boy+94]))
Given the generalized system, Σ_{P}, in Definition 3.7, the corresponding induced L_2-norm is evaluated as:

$$\sup_{\|\boldsymbol{w}\|_2 \neq 0} \frac{\|\boldsymbol{z}\|_2}{\|\boldsymbol{w}\|_2}$$

where the L_2-norm, $\|\boldsymbol{z}\|_2^2 = \int_0^\infty (\boldsymbol{z}^{\mathrm{T}}\boldsymbol{z})\mathrm{d}t$ and $\|\boldsymbol{w}\|_2^2 = \int_0^\infty (\boldsymbol{w}^{\mathrm{T}}\boldsymbol{w})\mathrm{d}t$ represents the energy associated with the controlled output and exogenous input signals, respectively.

Remark 3.6
The concept of $\mathcal{H}_\infty$-norm is defined only when dealing with LTI systems, while the L_2-norm is generally employed in the case of LPV systems. However, for LTI systems, the L_2 gain equals the $\mathcal{H}_\infty$-norm. Since LTI systems can be interpreted as 'frozen' realizations of a generic LPV system, the $\mathcal{H}_\infty$ criterion can be imposed through the minimization of the L_2-norm of the closed-loop system.

The control design based on the $\mathcal{H}_\infty$ criterion in Definition 3.8 aims at finding a controller that stabilizes the system by minimizing the sensitivity to any source of input disturbances, $\boldsymbol{w}$. In particular, the design targets the nominal stability and the nominal performance of the closed-loop system, Σ_{CL}, consisting of the interconnection between the generalized plant, Σ_{P}, and the LPV controller, $K(\boldsymbol{\rho})$. The properties of Σ_{CL} are shaped in the frequency domain through a set of weighting filters. By imposing conditions on the operating bandwidth and responsiveness of the system, it is possible to enhance the robustness of Σ_{CL} w.r.t. certain types of disturbances.

Definition 3.9 (Induced L_2-norm ($\mathcal{H}_\infty$) Control Problem)
Given an LPV closed-loop system, Σ_{CL}, resulting from the interconnection between a generalized LPV system, Σ_{P}, as in Definition 3.7, and an LPV controller, $K(\boldsymbol{\rho})$, as:

$$\Sigma_{\mathrm{CL}}: \begin{cases} \dot{\boldsymbol{x}}_{\mathrm{CL}}(t) = \mathcal{A}_{\mathrm{CL}}(\boldsymbol{\rho}(t))\boldsymbol{x}_{\mathrm{CL}}(t) + \mathcal{B}_{\mathrm{CL}}(\boldsymbol{\rho}(t))\boldsymbol{w}(t) \\ \boldsymbol{z}(t) \quad\;\; = \mathcal{C}_{\mathrm{CL}}(\boldsymbol{\rho}(t))\boldsymbol{x}_{\mathrm{CL}}(t) + \mathcal{D}_{\mathrm{CL}}(\boldsymbol{\rho}(t))\boldsymbol{w}(t) \end{cases} \tag{3.6}$$

where $\boldsymbol{x}_{\mathrm{CL}} = \left[\boldsymbol{x}_{\mathrm{P}}^{\mathrm{T}}, \boldsymbol{x}_K^{\mathrm{T}}\right]^{\mathrm{T}}$ is the state vector of the closed-loop system, which includes both the generalized LPV system and the controller state variables, $\boldsymbol{x}_{\mathrm{P}}$ and $\boldsymbol{x}_K$, respectively.

An $\mathcal{H}_\infty$ control problem consists of finding a controller, $K(\boldsymbol{\rho})$, that guarantees the LPV closed-loop system in Equation (3.6) to be robustly (or quadratically) stable, by minimizing the closed-loop system induced L_2-norm, computed as is Definition 3.8, as:

$$\min_{k(\boldsymbol{\rho}),\gamma_\infty} \text{ s.t. } \frac{\|\boldsymbol{z}\|_2}{\|\boldsymbol{w}\|_2} \leq \gamma_\infty$$

3.2.3.2 Grid-based Control Problem Formulation

Without loss of generality, consider a simplified parameterization of the generalized LPV plant described in Definition 3.7:

$$\Sigma_{\mathrm{P}}: \left[\begin{array}{c} \dot{\boldsymbol{x}}_{\mathrm{P}}(t) \\ \hline \begin{bmatrix} \boldsymbol{z}_1(t) \\ \boldsymbol{z}_2(t) \end{bmatrix} \\ \boldsymbol{y}(t) \end{array}\right] = \left[\begin{array}{c|cc} A(\boldsymbol{\rho}) & \begin{bmatrix} B_{11}(\boldsymbol{\rho}) & B_{12}(\boldsymbol{\rho}) \end{bmatrix} & B_2(\boldsymbol{\rho}) \\ \hline \begin{bmatrix} \mathcal{C}_{11}(\boldsymbol{\rho}) \\ \mathcal{C}_{12}(\boldsymbol{\rho}) \end{bmatrix} & \begin{bmatrix} 0 & 0 \\ 0 & 0 \end{bmatrix} & \begin{bmatrix} 0 \\ I_{n_{w_2}} \end{bmatrix} \\ C_2(\boldsymbol{\rho}) & \begin{bmatrix} 0 & I_{n_{z_2}} \end{bmatrix} & 0 \end{array}\right] \left[\begin{array}{c} \boldsymbol{x}_{\mathrm{P}}(t) \\ \hline \begin{bmatrix} \boldsymbol{w}_1(t) \\ \boldsymbol{w}_2(t) \end{bmatrix} \\ \boldsymbol{u}(t) \end{array}\right] \tag{3.7}$$

where the partitions $\boldsymbol{z}(t) = [\boldsymbol{z}_1(t), \boldsymbol{z}_2(t)]^{\mathrm{T}} \in \mathbb{R}^{n_z}$, $\boldsymbol{w}(t) = [\boldsymbol{w}_1(t), \boldsymbol{w}_2(t)]^{\mathrm{T}} \in \mathbb{R}^{n_w}$, $B_1(\boldsymbol{\rho}) = [B_{11}(\boldsymbol{\rho}), B_{12}(\boldsymbol{\rho})] \in \mathbb{R}^{n_{x_{\mathrm{P}}} \times n_w}$, and $C_1(\boldsymbol{\rho}) = [C_{11}(\boldsymbol{\rho}), C_{12}(\boldsymbol{\rho})]^{\mathrm{T}} \in \mathbb{R}^{n_z \times n_{x_{\mathrm{P}}}}$ hold, and assume $D_{11}(\boldsymbol{\rho}) = 0_{n_z \times n_w}$, $D_{22}(\boldsymbol{\rho}) = 0_{n_y \times n_u}$, $D_{12}(\boldsymbol{\rho}) \in \mathbb{R}^{n_z \times n_u}$ is full column rank, and $D_{21}(\boldsymbol{\rho}) \in \mathbb{R}^{n_y \times n_w}$ is full row rank for all $\boldsymbol{\rho}(t) \in \mathbb{U}_\rho$.

The following theorem provides the conditions to ensure the generalized LPV system in Equation (3.7) to be robustly stable in the sense of Definition 3.6, guaranteeing the induced L_2-norm performance of the resulting closed-loop system, through the resolution of the optimization problem in Definition 3.9.

Theorem 3.3 ([Wu+96])
Given a compact set $\mathbb{U}_\rho \subset \mathbb{R}^{n_\rho}$, non-negative numbers $\{\nu_i\}_{i=1}^{n_\rho}$, performance level γ, and the open-loop LPV system in Equation (3.7), the LPV synthesis γ-performance/ν-variation problem is solvable if and only if there exist continuously differentialble functions $X : \mathbb{R}^{n_\rho} \to \mathbb{R}^{n_{x_{\mathrm{P}}} \times n_{x_{\mathrm{P}}}}$ and $Y : \mathbb{R}^{n_\rho} \to \mathbb{R}^{n_{x_{\mathrm{P}}} \times n_{x_{\mathrm{P}}}}$, such that for all $\boldsymbol{\rho} \in \mathbb{U}_\rho$, $X(\boldsymbol{\rho})$, $Y(\boldsymbol{\rho}) > 0$, and:

$$\begin{bmatrix} Y(\boldsymbol{\rho})\hat{\mathcal{A}}^{\mathrm{T}}(\boldsymbol{\rho}) + \hat{\mathcal{A}}(\boldsymbol{\rho})Y(\boldsymbol{\rho}) - \sum_{i=1}^{n_\rho} \pm \left(\nu_i \frac{\partial Y(\boldsymbol{\rho})}{\partial \rho_i}\right) - \gamma \mathcal{B}_2(\boldsymbol{\rho})\mathcal{B}_2^{\mathrm{T}}(\boldsymbol{\rho}) & (\star)^{\mathrm{T}} & (\star)^{\mathrm{T}} \\ \mathcal{C}_{11}(\boldsymbol{\rho})Y(\boldsymbol{\rho}) & -\gamma I_{n_{z1}} & 0 \\ \mathcal{B}_1^{\mathrm{T}}(\boldsymbol{\rho}) & 0 & -\gamma I_{n_w} \end{bmatrix} \prec 0$$

$$\begin{bmatrix} \tilde{\mathcal{A}}^{\mathrm{T}}(\boldsymbol{\rho})X(\boldsymbol{\rho}) + X(\boldsymbol{\rho})\tilde{\mathcal{A}}(\boldsymbol{\rho}) - \sum_{i=1}^{n_\rho} \pm \left(\nu_i \frac{\partial X(\boldsymbol{\rho})}{\partial \rho_i}\right) - \gamma \mathcal{C}_2(\boldsymbol{\rho})\mathcal{C}_2^{\mathrm{T}}(\boldsymbol{\rho}) & (\star)^{\mathrm{T}} & (\star)^{\mathrm{T}} \\ \mathcal{B}_{11}^{\mathrm{T}}(\boldsymbol{\rho})X(\boldsymbol{\rho}) & -\gamma I_{n_{w1}} & 0 \\ \mathcal{C}_1^{\mathrm{T}}(\boldsymbol{\rho}) & 0 & -\gamma I_{n_z} \end{bmatrix} \prec 0$$

$$\begin{bmatrix} X(\boldsymbol{\rho}) & I_{n_x} \\ I_{n_x} & Y(\boldsymbol{\rho}) \end{bmatrix} \succeq 0$$

where:

$$\hat{\mathcal{A}}(\boldsymbol{\rho}) \coloneqq \mathcal{A}(\boldsymbol{\rho}) - \mathcal{B}_2(\boldsymbol{\rho})\mathcal{C}_{12}(\boldsymbol{\rho}); \qquad \tilde{\mathcal{A}}(\boldsymbol{\rho}) \coloneqq \mathcal{A}(\boldsymbol{\rho}) - \mathcal{B}_{12}(\boldsymbol{\rho})\mathcal{C}_2(\boldsymbol{\rho}).$$

The conditions in Theorem 3.3 define a standard infinite-dimensional LMIs problem. As

discussed in Section 3.2.2.1, the problem can be converted to a solvable finite-dimensional optimization by projecting the parameter-dependent Lyapunov functions, $X(\boldsymbol{\rho})$ and $Y(\boldsymbol{\rho})$, on a finite set of n_{B} basis functions, as in Theorem 3.1, and by dicretizing the continuous space of variation of the parameters into a finite grid of n_{g} values of $\boldsymbol{\rho} \in \bar{\mathbb{U}}_{\rho}$, as in Proposition 3.1. Thus, by parametrizing the Lyapunov functions through sets of scalar differentiable basis functions, $\{f_i : \mathbb{R}^{n_p} \to \mathbb{R}\}_{i=1}^{n_{\mathrm{B}}}$ and $\{g_i : \mathbb{R}^{n_p} \to \mathbb{R}\}_{i=1}^{n_{\mathrm{B}}}$, as:

$$X(\boldsymbol{\rho}) = X_0 + \sum_{i=1}^{n_{\mathrm{B}}} f_i(\boldsymbol{\rho}) X_i; \qquad Y(\boldsymbol{\rho}) = Y_0 + \sum_{i=1}^{n_{\mathrm{B}}} g_i(\boldsymbol{\rho}) Y_i \tag{3.8}$$

where $X_0, X_i \in \mathbb{R}^{n_{x_{\mathrm{P}}} \times n_{x_{\mathrm{P}}}}$ and $Y_0, Y_i \in \mathbb{R}^{n_{x_{\mathrm{P}}} \times n_{x_{\mathrm{P}}}}$, the resulting finite-dimensional control synthesis problem can be formulated as it follows.

Proposition 3.2 ($\mathcal{H}_\infty$ Dynamic Output-Feedback Control Problem)
Given the LPV closed-loop system, Σ_{CL}, in Equation (3.6), a dynamic output-feedback control problem consists of finding a controller, $K(\boldsymbol{\rho})$, that solves the $\mathcal{H}_\infty$ control problem in Definition 3.9 (guaranteeing robust stability), by satisfying the LMIs conditions derived in Theorem 3.3. According to the formulation in Theorem 3.3, the LPV controller is parameterized as:

$$K(\boldsymbol{\rho}) : \begin{bmatrix} \dot{\boldsymbol{x}}_K(t) \\ \boldsymbol{u}(t) \end{bmatrix} = \begin{bmatrix} \mathcal{A}_K(\boldsymbol{\rho}) & \mathcal{B}_K(\boldsymbol{\rho}) \\ \mathcal{C}_K(\boldsymbol{\rho}) & \mathcal{D}_K(\boldsymbol{\rho}) \end{bmatrix} \begin{bmatrix} \boldsymbol{x}_K(t) \\ \boldsymbol{y}(t) \end{bmatrix} \tag{3.9}$$

where:

$$\begin{aligned}
\mathcal{A}_K(\boldsymbol{\rho}, \dot{\boldsymbol{\rho}}) &\coloneqq \big[\mathcal{A}(\boldsymbol{\rho}) + \gamma^{-1}[Q^{-1}(\boldsymbol{\rho})X(\boldsymbol{\rho})L(\boldsymbol{\rho})\mathcal{B}_{12}^{\mathrm{T}} + \mathcal{B}_1(\boldsymbol{\rho})\mathcal{B}_1^{\mathrm{T}}(\boldsymbol{\rho})]Y^{-1}(\boldsymbol{\rho}) \\
&\qquad + \mathcal{B}_2(\boldsymbol{\rho})F(\boldsymbol{\rho}) + Q^{-1}(\boldsymbol{\rho})X(\boldsymbol{\rho})L(\boldsymbol{\rho})\mathcal{C}_2(\boldsymbol{\rho}) - Q^{-1}(\boldsymbol{\rho})H(\boldsymbol{\rho}, \dot{\boldsymbol{\rho}})\big], \\
\mathcal{B}_K(\boldsymbol{\rho}) &\coloneqq -\big[Q^{-1}(\boldsymbol{\rho})X(\boldsymbol{\rho})L(\boldsymbol{\rho})\big], \\
\mathcal{C}_K(\boldsymbol{\rho}) &\coloneqq F(\boldsymbol{\rho}),
\end{aligned}$$

and:

$$\begin{aligned}
Q(\boldsymbol{\rho}) &\coloneqq \big[X(\boldsymbol{\rho}) - Y(\boldsymbol{\rho})^{-1}\big], \\
F(\boldsymbol{\rho}) &\coloneqq -\big[\gamma\mathcal{B}_2^{\mathrm{T}}(\boldsymbol{\rho})Y^{-1}(\boldsymbol{\rho}) + \mathcal{C}_{12}(\boldsymbol{\rho})\big], \\
L(\boldsymbol{\rho}) &\coloneqq -\big[\gamma X^{-1}\mathcal{C}_2^{\mathrm{T}}(\boldsymbol{\rho}) + \mathcal{B}_{12}(\boldsymbol{\rho})\big], \\
H(\boldsymbol{\rho}, \dot{\boldsymbol{\rho}}) &\coloneqq -\Bigg[\mathcal{A}_F^{\mathrm{T}}(\boldsymbol{\rho})Y^{-1} + Y^{-1}\mathcal{A}_F(\boldsymbol{\rho}) + \sum_i \left(\dot{\boldsymbol{\rho}}\frac{\partial Y^{-1}}{\partial \boldsymbol{\rho}}\right) \\
&\qquad + \gamma^{-1}\mathcal{C}_F^{\mathrm{T}}(\boldsymbol{\rho})\mathcal{C}_F(\boldsymbol{\rho}) + \gamma^{-1}Y^{-1}(\boldsymbol{\rho})\mathcal{B}_1(\boldsymbol{\rho})\mathcal{B}_1^{\mathrm{T}}(\boldsymbol{\rho})Y^{-1}(\boldsymbol{\rho})\big],
\end{aligned}$$

with:

$$\mathcal{A}_F(\boldsymbol{\rho}) \coloneqq \mathcal{A}(\boldsymbol{\rho}) + \mathcal{B}_2(\boldsymbol{\rho})F(\boldsymbol{\rho}); \qquad \mathcal{C}_F^{\mathrm{T}}(\boldsymbol{\rho}) \coloneqq \big[\mathcal{C}_{11}^{\mathrm{T}}(\boldsymbol{\rho}) \;\; \mathcal{C}_{12}^{\mathrm{T}}(\boldsymbol{\rho}) + F^{\mathrm{T}}(\boldsymbol{\rho})\big].$$

The solution to the problem consists of a set of n_{g} LTI realizations of the LPV controller in Equation (3.9), evaluated at each selected grid point for frozen values of $\boldsymbol{\rho} \in \bar{\mathbb{U}}_{\rho}$. The implementation of the LPV controller for any intermediate scheduling variables' values relies on the linear interpolation between the LTI set.

3.2.3.3 Polytopic Control Problem Formulation

As previously mentioned in Chapter 2, the control-oriented formulation of an LPV polytopic system is based on an affine model-parameters relation, as in Definition 2.4. In order to respect the affine condition through the formulation of the LMIs controller synthesis problem, the following assumptions have to be imposed.

Assumption 3.1 ((A1) in [AGB95])
The generalized LPV plant must be strictly proper, hence $\mathcal{D}_{22}(\boldsymbol{\rho}) = 0$.

Assumption 3.2 ((A2) in [AGB95])
The input/output matrices, $\mathcal{B}_2(\boldsymbol{\rho})$, $\mathcal{C}_2(\boldsymbol{\rho})$, $\mathcal{D}_{12}(\boldsymbol{\rho})$, $\mathcal{D}_{21}(\boldsymbol{\rho})$, *must be parameter-independent.*

Based on Assumptions 3.1-3.2, the generalized LPV plant described in Definition 3.7, has to be reformulated as:

$$\Sigma_{\mathrm{P}} : \begin{bmatrix} \dot{\boldsymbol{x}}_{\mathrm{P}}(t) \\ \hline \boldsymbol{z}(t) \\ \boldsymbol{y}(t) \end{bmatrix} = \left[\begin{array}{c|cc} \mathcal{A}(\rho) & \mathcal{B}_1(\boldsymbol{\rho}) & \mathcal{B}_2 \\ \hline \mathcal{C}_1(\boldsymbol{\rho}) & \mathcal{D}_{11}(\boldsymbol{\rho}) & \mathcal{D}_{12} \\ \mathcal{C}_2 & \mathcal{D}_{21} & 0 \end{array}\right] \begin{bmatrix} \boldsymbol{x}_{\mathrm{P}}(t) \\ \hline \boldsymbol{w}(t) \\ \boldsymbol{u}(t) \end{bmatrix} \tag{3.10}$$

The following propositions provide the sufficient conditions to ensure the generalized LPV system in Equation (3.10) is quadratically stable in the sense of Definition 3.5. The formulation guarantees the induced L_2-norm performance of the resulting closed-loop system, through the resolution of the optimization problem in Definition 3.9, by employing a polytopic approach. The LMIs conditions have been derived in [SGC97] and reformulated as in [PV08], where additional details and related proofs of the propositions are discussed.

Proposition 3.3 (Feasibility - $\mathcal{H}_\infty$ Polytopic Control Problem)
Consider the LPV closed-loop system, Σ_{CL}, *in Equation* (3.6), *where the generalized open-loop system,* Σ_{P}, *in Equation* (3.10), *is formulated as the LPV polytopic system in Equation* (2.4). *There exists a full-order dynamic output feedback controller,* $K(\boldsymbol{\rho})$, *that solves the* $\mathcal{H}_\infty$ *control problem in Definition 3.9 (guaranteeing quadratic stability), if there exist symmetric matrices,* $X, Y \in \mathbb{R}^{n_{x_{\mathrm{P}}} \times n_{x_{\mathrm{P}}}}$, *and matrices* $\tilde{\mathcal{A}}(\boldsymbol{\theta}_i) \in \mathbb{R}^{n_{x_{\mathrm{P}}} \times n_{x_{\mathrm{P}}}}$, $\tilde{\mathcal{B}}(\boldsymbol{\theta}_i) \in \mathbb{R}^{n_{x_{\mathrm{P}}} \times n_y}$, $\tilde{\mathcal{C}}(\boldsymbol{\theta}_i) \in \mathbb{R}^{n_u \times n_{x_{\mathrm{P}}}}$, $\tilde{\mathcal{D}}(\boldsymbol{\theta}_i) \in \mathbb{R}^{n_u \times n_y}$, *and a performance level* $\gamma > 0 \in \mathbb{R}$, *such that:*

$$\begin{bmatrix} M_{11} & (\star)^{\mathrm{T}} & (\star)^{\mathrm{T}} & (\star)^{\mathrm{T}} \\ M_{21} & M_{22} & (\star)^{\mathrm{T}} & (\star)^{\mathrm{T}} \\ M_{31} & M_{32} & -\gamma I_{n_w} & (\star)^{\mathrm{T}} \\ M_{41} & M_{42} & M_{43} & -\gamma I_{n_z} \end{bmatrix} \prec 0$$
$$\begin{bmatrix} X & I_{n_{x_{\mathrm{P}}}} \\ I_{n_{x_{\mathrm{P}}}} & Y \end{bmatrix} \succ 0 \tag{3.11}$$

where:

$$
\begin{aligned}
M_{11} &\coloneqq \mathcal{A}(\boldsymbol{\theta}_i)X + X\mathcal{A}^{\mathrm{T}}(\boldsymbol{\theta}_i) + \mathcal{B}_2\tilde{\mathcal{C}}(\boldsymbol{\theta}_i) + \tilde{\mathcal{C}}^{\mathrm{T}}(\boldsymbol{\theta}_i)\mathcal{B}_2^{\mathrm{T}} \\
M_{21} &\coloneqq \tilde{\mathcal{A}}(\boldsymbol{\theta}_i) + \mathcal{A}^{\mathrm{T}}(\boldsymbol{\theta}_i) + \mathcal{C}_2^{\mathrm{T}}\tilde{\mathcal{D}}^{\mathrm{T}}(\boldsymbol{\theta}_i)\mathcal{B}_2^{\mathrm{T}} \\
M_{22} &\coloneqq Y\mathcal{A}(\boldsymbol{\theta}_i) + \mathcal{A}^{\mathrm{T}}(\boldsymbol{\theta}_i)Y + \tilde{\mathcal{B}}(\boldsymbol{\theta}_i)\mathcal{C}_2 + \mathcal{C}_2^{\mathrm{T}}\tilde{\mathcal{B}}^{\mathrm{T}}(\boldsymbol{\theta}_i) \\
M_{31} &\coloneqq \mathcal{B}_1^{\mathrm{T}}(\boldsymbol{\theta}_i) + \mathcal{D}_{21}^{\mathrm{T}}\tilde{\mathcal{D}}^{\mathrm{T}}(\boldsymbol{\theta}_i)\mathcal{B}_2^{\mathrm{T}} \\
M_{32} &\coloneqq \mathcal{B}_1^{\mathrm{T}}(\boldsymbol{\theta}_i)Y + \mathcal{D}_{21}^{\mathrm{T}}\tilde{\mathcal{B}}^{\mathrm{T}}(\boldsymbol{\theta}_i) \\
M_{41} &\coloneqq \mathcal{C}_1(\boldsymbol{\theta}_i)X + \mathcal{D}_{12}\tilde{\mathcal{C}}(\boldsymbol{\theta}_i) \\
M_{42} &\coloneqq \mathcal{C}_1(\boldsymbol{\theta}_i) + \mathcal{D}_{12}\tilde{\mathcal{D}}(\boldsymbol{\theta}_i)\mathcal{C}_2 \\
M_{43} &\coloneqq \mathcal{D}_{11}(\boldsymbol{\theta}_i) + \mathcal{D}_{12}\tilde{\mathcal{D}}(\boldsymbol{\theta}_i)\mathcal{D}_{21}
\end{aligned}
$$

hold at each vertex, $\boldsymbol{\theta}_i = [\nu_{i,1}, \ldots, \nu_{i,n_\rho}]$, of the polytope, where $\nu_{i,j}$ is the j^{th} scheduling variables that equals either the upper or the lower bounds, $\overline{\rho_j}$ and $\underline{\rho_j}$, respectively.

Proposition 3.4 (Reconstruction - $\mathcal{H}_\infty$ Polytopic Control Problem)
If the conditions in Proposition 3.3 are fulfilled, then the controller, $K(\boldsymbol{\rho})$ exitsts and can be expressed as:

$$
K(\boldsymbol{\rho}) : \begin{bmatrix} \dot{\boldsymbol{x}}_K(t) \\ \boldsymbol{u}(t) \end{bmatrix} = \begin{bmatrix} \mathcal{A}_K(\boldsymbol{\rho}) & \mathcal{B}_K(\boldsymbol{\rho}) \\ \mathcal{C}_K(\boldsymbol{\rho}) & \mathcal{D}_K(\boldsymbol{\rho}) \end{bmatrix} \begin{bmatrix} \boldsymbol{x}_K(t) \\ \boldsymbol{y}(t) \end{bmatrix} \tag{3.12}
$$

The controller reconstruction is obtained by solving the following system of equations at each vertex, $\boldsymbol{\theta}_i = [\nu_{i,1}, \ldots, \nu_{i,n_\rho}]$, of the polytope, where $\nu_{i,j}$ is the j^{th} scheduling variables that equals either the upper or the lower bounds, $\overline{\rho_j}$ and $\underline{\rho_j}$, respectively:

$$
\begin{aligned}
\mathcal{D}_K(\boldsymbol{\theta}_i) &\coloneqq \tilde{\mathcal{D}}(\boldsymbol{\theta}_i) \\
\mathcal{C}_K(\boldsymbol{\theta}_i) &\coloneqq \Big(\tilde{\mathcal{C}}(\boldsymbol{\theta}_i) - \mathcal{D}_K(\boldsymbol{\theta}_i)\mathcal{C}_2 X\Big) M^{-\mathrm{T}} \\
\mathcal{B}_K(\boldsymbol{\theta}_i) &\coloneqq N^{-1}\Big(\tilde{\mathcal{B}}(\boldsymbol{\theta}_i)) - Y\mathcal{B}_2\mathcal{D}_K(\boldsymbol{\theta}_i)\Big) \\
\mathcal{A}_K(\boldsymbol{\theta}_i) &\coloneqq N^{-1}\Big(\tilde{\mathcal{A}}(\boldsymbol{\theta}_i) - Y\mathcal{A}(\boldsymbol{\theta}_i)X - Y\mathcal{B}_2\mathcal{D}_K(\boldsymbol{\theta}_i)\mathcal{C}_2 X \\
&\qquad\qquad - N\mathcal{B}_K(\boldsymbol{\theta}_i)\mathcal{C}_2 X - Y\mathcal{B}_2\mathcal{C}_K(\boldsymbol{\theta}_i)M^{\mathrm{T}}\Big) M^{-\mathrm{T}}
\end{aligned}
$$

where M and N are defined such that $MN^{\mathrm{T}} = I_{n_{x_{\mathrm{P}}}} - XY$, which are chosen by applying a Singular Value Decomposition (SVD) and a Cholesky factorization.

The solution of the control problem in Proposition 3.4 consists of a set of LTI realizations of the LPV controller in Equation (3.12), evaluated at each vertex of the polytope, $\boldsymbol{\theta}_i \in \Theta$. Since the controllers share the same constant Lyapunov functions, X and Y, quadratic stability properties are ensured across the entire convex subspace described by the polytope. As a drawback, the controller relies on a sub-optimal solution of the LMIs optimization problem in Equation (3.11), solved at each vertex of the polytope, introducing a certain degree of conservatism in the controller synthesis performance.

3.3 Polytopic Controller Design

In this section, the synthesis of the LPV polytopic controller, K_{PY}, is presented. The controller synthesis is based on the approximated LPV polytopic model of the projectile pitch channel dynamics derived in Chapter 2, Section 2.4. The generalized plant architecture is first introduced, defying the core objectives of the design. The controller synthesis addresses the flight envelope represented by the variation of the original scheduling variables: $\alpha \in [0, 16]$ deg, $V \in [160, 280]$ m/s, and $h \in [1, 15]$ km. However, the actual design polytope, $\hat{\Theta}$, is defined through the corresponding ranges of variation of the identified set of scheduling functions ($\hat{\rho}_1$, $\hat{\rho}_2$, $\hat{\rho}_3$), obtained in Section 2.4, as a result of the approximation process.

Prior to the controller synthesis, the dimensions of the polytope are analyzed in detail and iteratively optimized, in order to minimize the conservatism affecting the optimization problem. Indeed, the polytope mapping process developed in Section 2.4.2 resulted in the identification of a convex space that is larger than the original flight envelope. The iterative computation of the controller design, and the analysis of the resulting performance in time simulations, allows for progressively adjusting the ranges of variation of $\hat{\rho}_1$, $\hat{\rho}_2$, and $\hat{\rho}_3$ that define the polytope, $\hat{\Theta}$. The final results of the design process are investigated in the frequency domain to assess the properties of the closed-loop system in terms of reference tracking and disturbance rejection capabilities.

3.3.1 Polytopic Design Scheme

The design architecture employed for the controller synthesis is presented in Figure 3.1 and complies with the generalized system formulation expressed in Equation (3.10). The second-order actuator model, T_{act}, presented in Equation (1.39) of Chapter 1, is included in the definition of the generalized plant to account for the actuator dynamics, together with the projectile polytopic quasi-LPV model, Σ_{PY}, summarized in Equation (2.42), in the conclusions of Chapter 2. A set of first-order weighting functions, W_e and W_u, imposes the desired closed-loop tracking capability and control effort performances in the frequency domain, by targeting the corresponding tracking error, $e = r - \alpha$, and the derivative of the control deflection input, $\dot{\delta}_{q,\mathrm{cmd}}$. The reference signal, r, consists of an AoA trajectory defined through an LDR optimization law ([Phi08]; [KCL82]). The weighting functions are parametrized as:

$$W_e(s) = \frac{s/M_e + \omega_e}{s + \omega_e \epsilon_e}; \qquad W_u(s) = \frac{s + \omega_u/M_u}{\epsilon_u s + \omega_u}$$

where the high-frequency gain, $M_e = 2$, the low-frequency gain, $\epsilon_e = 0.01$, and the crossover frequency, $\omega_e = 1$ rad/s, are selected respectively to guarantee 6 dB of module margin for robustness purposes, -40 dB of disturbance attenuation, and a steady-state tracking error $\leq 1\%$ at low frequency. Similarly, $M_u = 5.5$, $\epsilon_u = 0.01$, and $\omega_u = 100$ rad/s provide respectively a maximum 15 dB low-frequency gain, -40 dB of noise attenuation, and an input bandwidth that complies with the actuator operating limitations, aiming to prevent stall regime occurrence.

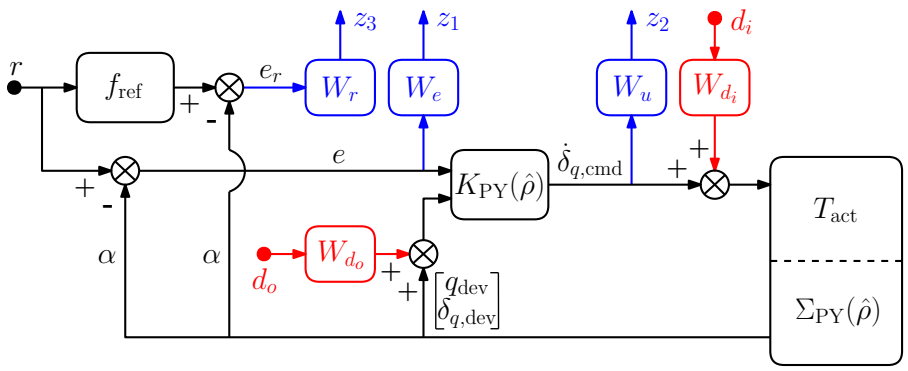

Figure 3.1: Polytopic design scheme architecture.

Since tracking capability and disturbance rejection are demanding properties, the imposition of a single filter cannot simultaneously optimize both. The bandwidth of W_e is dedicated to ensuring a reliable output disturbance rejection to the system, while an additional first-order weighting function, W_r, imposes larger bandwidth requirements to improve the tracking response. The weighting function is applied to the response error, $e_r = f_{\text{ref}} - \alpha$, evaluated as the difference between the tracking response of a desired reference model, f_{ref}, and the tracking response of the projectile dynamics.

A core objective of the reference model selection relies on minimizing the overshoot affecting the system response. Indeed, in a gliding flight scenario, the guidance reference signal is generally engaged at the apogee of the projectile's trajectory, generating sudden and sharp variations in the projectile's attitude. A large overshoot on the AoA might lead to the saturation of the aerodynamic control surfaces, critical for control purposes. As a consequence, the first-order reference model, and the related tracking response weighting function are parametrized respectively as:

$$f_{\text{ref}}(s) = \frac{\omega_f}{s + \omega_f}; \qquad W_r(s) = \frac{s/M_r + \omega_r}{s + \omega_r \epsilon_r};$$

where the $\omega_f = 10$ rad/s, $M_r = 2$, $\epsilon_r = 0.001$, and $\omega_r = 10$ rad/s, coherently.

Constant weights, $W_{d_i} = 0.6$ and $W_{d_o} = 0.2$, are also applied to the input and output disturbance signals, d_i and d_o respectively, aiming to properly scale the disturbance effects on the model dynamics.

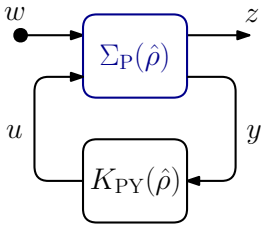

Figure 3.2: General polytopic control scheme configuration.

Remark 3.7
The weighting functions are designed independently of the scheduling functions in $\hat{\rho}(t)$, meaning that the same performances are imposed at each vertex condition of the polytope, leading to possible conservativeness in the synthesis results.

The control scheme in Figure 3.1 is then generalized as in Figure 3.2, where the LPV plant, $\Sigma_{\mathrm{P}}(\hat{\rho})$, includes the dynamics of the actuator, the projectile polytopic model, the reference model, and the weighting functions. Thus, according to the generalized polytopic plant formulation in Equation (3.10), the overall generalized state vector is defined as: $\boldsymbol{x}_{\mathrm{P}} = [\boldsymbol{x}^{\mathrm{T}}, \boldsymbol{x}_{\mathrm{act}}^{\mathrm{T}}, x_{f_{\mathrm{ref}}}, x_{W_e}, x_{W_u}, x_{W_r}]^{\mathrm{T}} \in \mathbb{R}^9$, with $\boldsymbol{x} = [\alpha, q_{\mathrm{dev}}, \delta_{q,\mathrm{dev}}]^{\mathrm{T}} \in \mathbb{R}^3$. The generalized exogenous input vector, $\boldsymbol{w} = [r, d_i, d_o]^{\mathrm{T}} \in \mathbb{R}^3$, accounts for the reference guidance signal and the input and output disturbances, while the generated control input, $u \in \mathbb{R}$, corresponds to the commanded virtual pitch deflection rate, $\dot{\delta}_{q,\mathrm{cmd}}$, imposed on the canards. Indeed, the inclusion of the integrator dynamics during the state transformation process resulted in the redefinition of the quasi-LPV model input, σ, as the derivative of δ_q. Finally, the generalized controlled output vector, $\boldsymbol{z} = [z_1, z_2, z_3]^{\mathrm{T}} \in \mathbb{R}^3$, includes the control optimization objectives, while the set of available measurements, $\boldsymbol{y} = [e, q_{\mathrm{dev}}, \delta_{q,\mathrm{dev}}]^{\mathrm{T}} \in \mathbb{R}^3$, is the controller input.

The generalized plant is then evaluated at each vertex of the polytope, $\hat{\boldsymbol{\theta}}_i \in \hat{\Theta}$ with $i = 1, \ldots, 8$, by substituting the corresponding values of the scheduling functions. The resulting LTI system realizations are employed in the resolution of the set of LMIs that defines the polytopic controller synthesis problem, formulated in Propositions 3.3-3.4.

3.3.2 Polytope Reduction Analysis

The mapping process developed in Chapter 2, Section 2.4.2 allowed defining the polytope's dimensions through the identification of the scheduling functions' variation ranges: $\hat{\rho}_1 \in [0.4, 2.9] \times 10^4$, $\hat{\rho}_2 \in [0.05, 0.55]$, and $\hat{\rho}_3 \in [-1, 4.1]$. As mentioned at the end of Section 2.4.2, the polytope definition is affected by a certain level of conservatism due to the limited accuracy of the flight conditions selection criteria. Consequently, the controller synthesis might account for areas of the flight envelope that are unfeasible for the specific gliding-phase trajectory targeted by the design, over-constraining the optimization problem. In order to optimize the dimensions of the polytope, the variation of each scheduling function, $(\hat{\rho}_1, \hat{\rho}_2, \hat{\rho}_3)$, is investigated across the original projectile's flight envelope: $\alpha \in [0, 16]$ deg, $V \in [160, 280]$ m/s, and $h \in [1, 15]$ km. The analysis aims to identify any unfeasible operating conditions, (α, V, h), generated by the polytope mapping process. Additionally, by iteratively performing the controller synthesis on a progressively optimized convex space, the polytope's dimensions can be properly adjusted to comply with the desired gliding-phase trajectory of the projectile.

Aiming for a clearer understanding of the relation between the original and the newly identified convex spaces, the variation of the scheduling functions is evaluated across the flight domain of each scheduling variable (α, V, h). The results in Figure 3.3 show the mutual dependence of the scheduling functions on the altitude variation. In particular, both $\hat{\rho}_1$ and $\hat{\rho}_2$ present higher values at lower altitude levels, and vice versa, as observed in Figure 3.3(a).

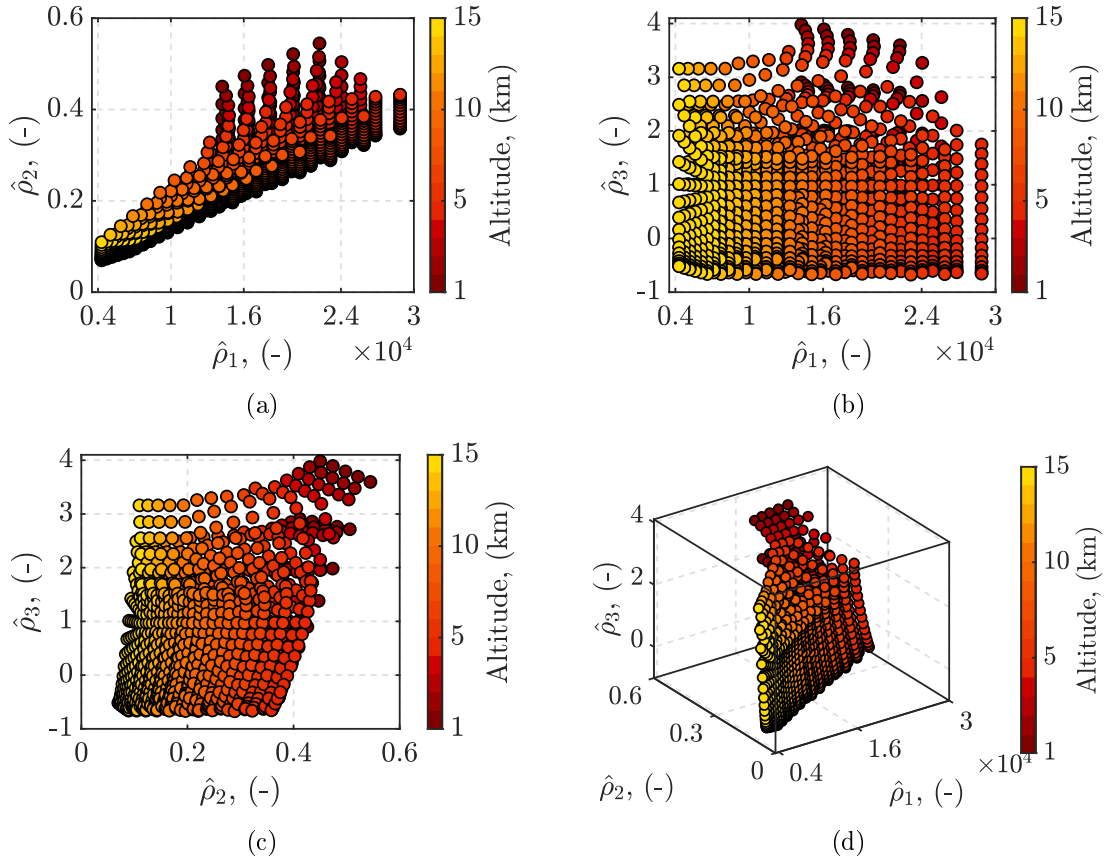

Figure 3.3: Dependence on the altitude: (a) $\hat{\rho}_1$-$\hat{\rho}_2$; (b) $\hat{\rho}_1$-$\hat{\rho}_3$; (c) $\hat{\rho}_2$-$\hat{\rho}_3$; (d) 3D space.

Differently, Figures 3.3(b)-(c) reveal the nearly independent relation of $\hat{\rho}_3$ to the altitude level. In the following, in order to simplify the analysis of the remaining scheduling variables, α and V, only a subspace of the flight envelope is investigated, belonging to a fixed altitude level: $h = 7$ km. Indeed, the results obtained across the full envelope confirmed that the dependence on the scheduling functions on α and V is not affected by the altitude level.

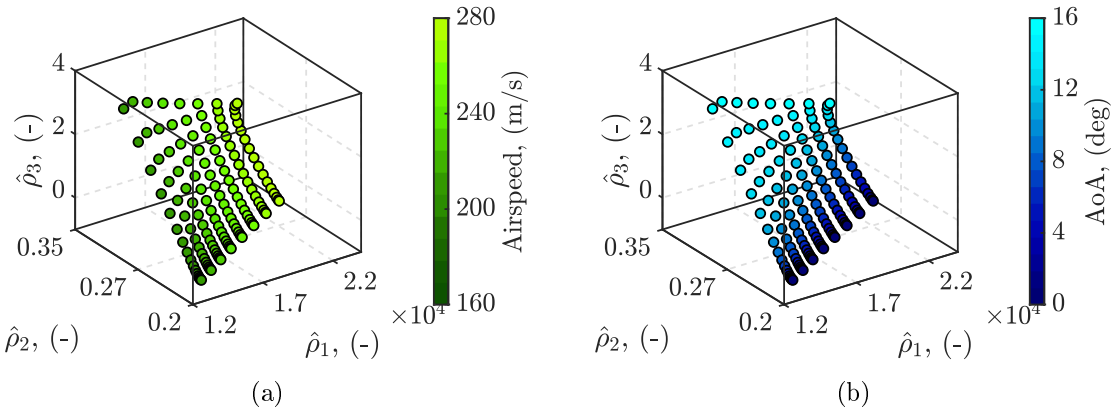

Figure 3.4: Polytope's 3D dimensions dependence: (a) airspeed; (b) AoA.

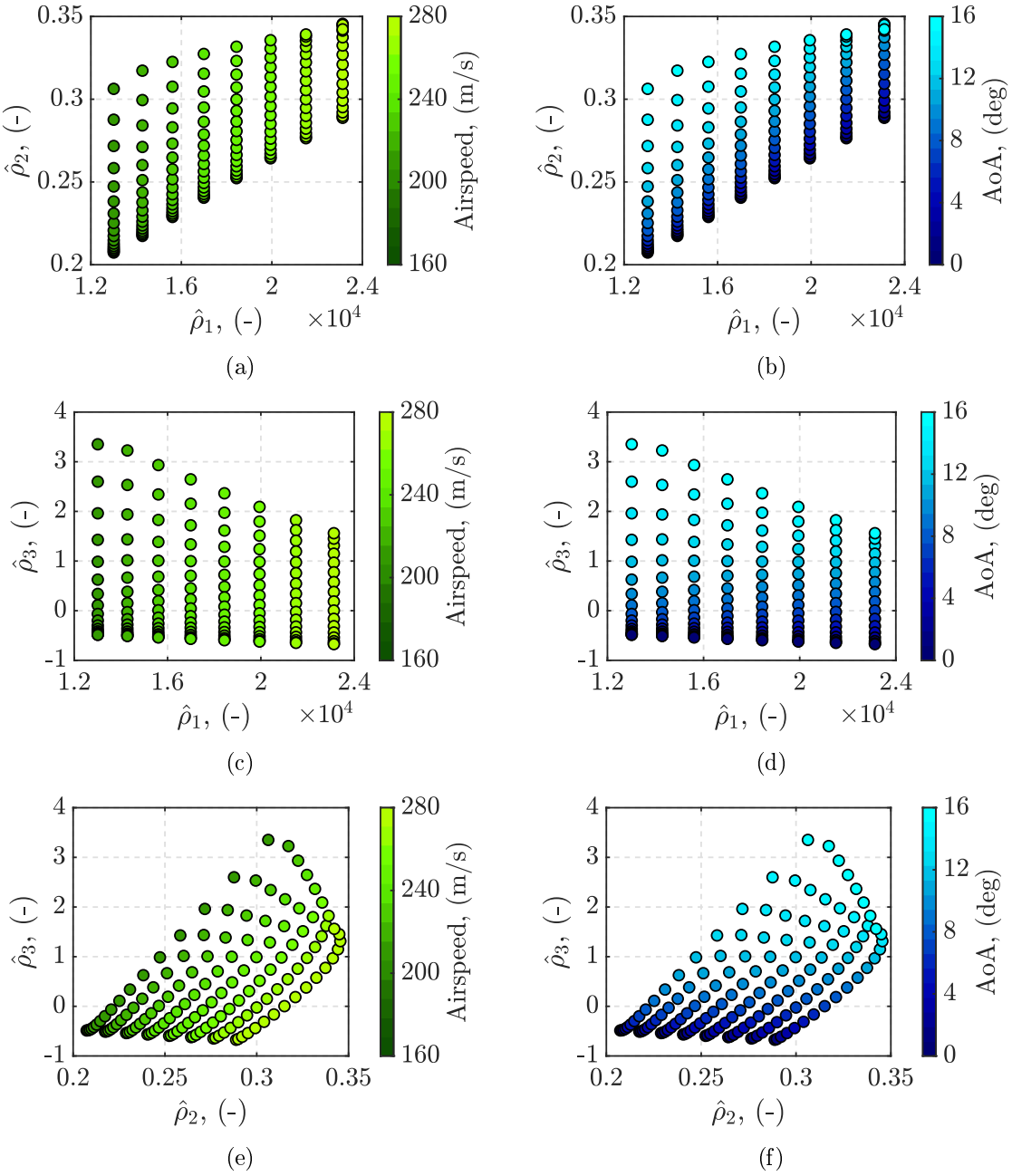

Figure 3.5: Polytope's dimensions dependence on the airspeed and AoA variations: (a)-(b) $\hat{\rho}_1$-$\hat{\rho}_2$, respectively; (c)-(d) $\hat{\rho}_1$-$\hat{\rho}_3$, respectively; (e)-(f) $\hat{\rho}_2$-$\hat{\rho}_3$, respectively.

The results in Figure 3.4 and Figure 3.5 provide a comparison between the mutual dependence of the scheduling functions to the scheduling variables, α and V. As expected, $\hat{\rho}_1$ presents an evident dependence on the airspeed, while it results completely independent of the AoA. Indeed, through the polytopic modeling procedure developed in Chapter 2, $\hat{\rho}_1$ has been defined as the dynamic pressure. On the other hand, the complex parameterizations of the remaining scheduling functions, $\hat{\rho}_2$ and $\hat{\rho}_3$, prevent a straightforward intuition about their

variations across the flight envelope. The analyses in Figures 3.5(d)(f) reveal a relevant dependence of $\hat{\rho}_3$ to the AoA variation, while the effect of the airspeed conditions in Figures 3.5(c)(e) appears to be almost negligible. Conversely, the variation of $\hat{\rho}_2$ is characterized by a strong dependence on the airspeed conditions, as in Figures 3.5(a)(e), and a negligible dependence on AoA values. Indeed, the apparent relation shown in Figures 3.5(b)(f) is clarified by the 3D representation in Figure 3.4(b), where the higher values of $\hat{\rho}_2$ only occur for corresponding higher values of $\hat{\rho}_3$ (highly dependent on the AoA).

The observations provided by the different analyses highlighted potential areas of the polytope characterized by unfeasible flight conditions. Indeed, at low altitude levels, $h \leq 3$ km, high values of airspeed are very unlikely to occur, and vice versa, combinations of $h \geq 10$ km and low airspeed regime are not feasible for the projectile's gliding trajectory. The refinement of the variation ranges of $\hat{\rho}_1$, $\hat{\rho}_2$, and $\hat{\rho}_3$, is based on the knowledge acquired through the polytope analyses, and the iterative performance of trajectory simulations of progressively more accurate LPV controllers. As will be shown in the simulation results presented in Chapter 4, the actual area covered by the scheduling functions' trajectories belongs to a bounded subspace of the polytope, $\hat{\Theta}$, identified in Chapter 2. In particular, the limitations imposed on the control effort through the controller design, preventing possible canards saturation, drastically reduced the available AoA variation range and consequently the $\hat{\rho}_3$ boundaries.

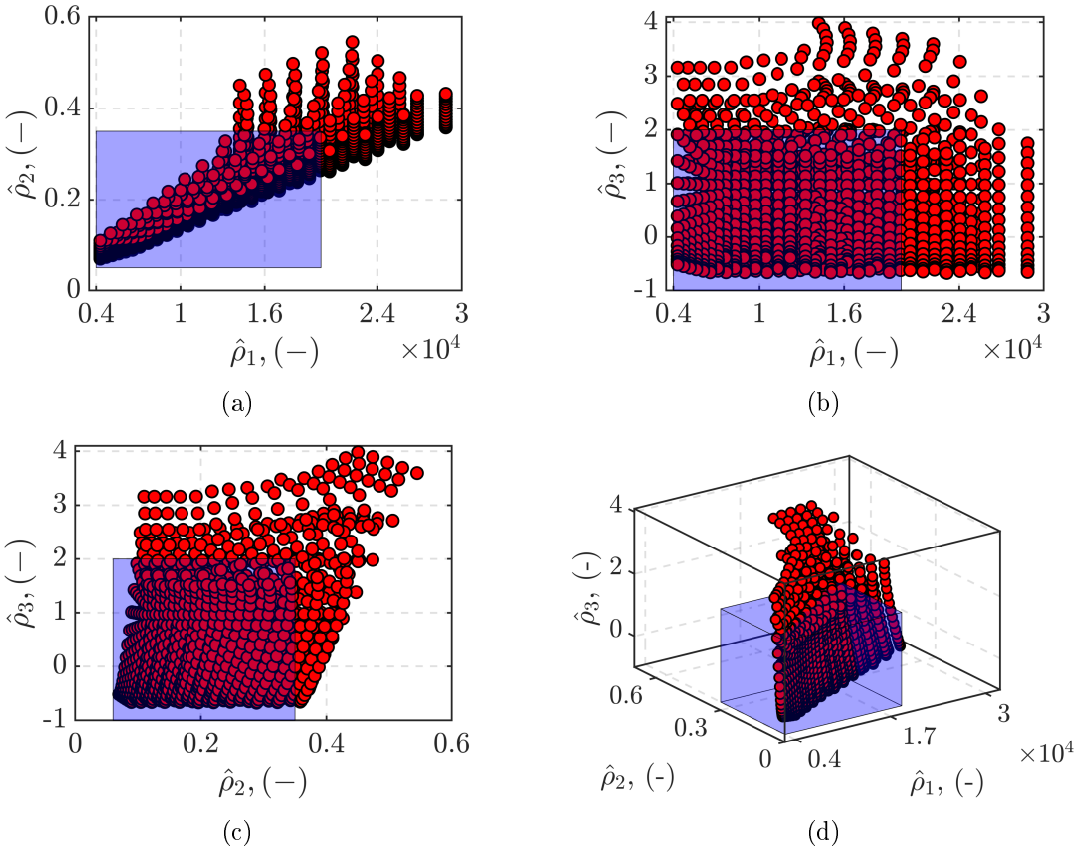

Figure 3.6: Reduced polytope $\hat{\Theta}_{\mathrm{R}}$: (a) $\hat{\rho}_1$-$\hat{\rho}_2$; (b) $\hat{\rho}_1$-$\hat{\rho}_3$; (c) $\hat{\rho}_2$-$\hat{\rho}_3$; (d) 3D space.